The characterization of endosomal insulin degradation intermediates and their sequence of production

Paul J. SEABRIGHT and Geoffrey D. SMITH*

University of Cambridge, Department of Clinical Biochemistry, Addenbrooke's Hospital, Hills Road, Cambridge CB2 2QR, U.K.

Insulin degradation within isolated rat liver endosomes was studied *in vitro* with the aid of three ^{125}I-insulin isomers specifically labelled at tyrosine (A14, B16 and B26). Chloroquine and 1,10-phenanthroline were used to minimize insulin proteolysis during endosome preparation, whereas the manipulation of endosomal processing of insulin *in vitro* by Co^{2+} ions (to activate) and 1,10-phenanthroline (to inhibit) permitted the study of degradation intermediates and their time-dependent production. Structural and kinetic analysis of intermediates isolated from both intra- and extra-endosomal compartments allowed the determination of major cleavage sites and the probable sequence of proteolytic events. It was found that ^{125}I-tyrosine is the ultimate labelled degradation product of all iodo-insulin isomers, suggesting that endosomal proteases are able to degrade insulin to the level of its constituent amino acids. ^{125}I-tyrosine was also the only radiolabelled product able to cross the endosomal membrane. Intra-endosomal insulin degradation proceeds via two inter-related cleavage routes after metalloendoprotease cleavage of the B-chain. One pathway results from an initial cleavage in the centre region of the B-chain (B7–19), probably at B14-15, whereas the major route results from a cleavage at B24-25. B24-25 cleavage removes the B-chain C-terminal hexapeptide (B25–30), which is subsequently cleaved by an aminopeptidase activity to produce first the pentapeptide B26–30 and then ^{125}I-tyrosine. The isolation of intact radiolabelled A-chain from the degradation of ^{125}I-[A14]-insulin suggests that further degradation of proteolytic intermediates containing cleaved B-chain proceeds via interchain disulphide reduction. The A-chain is then processed by several cleavages, one of which occurs at A13-14.

INTRODUCTION

Insulin binds to its receptor at the plasma membrane, which initiates receptor autophosphorylation [1] and activation of the intrinsic tyrosine kinase [2], thus triggering the signal transduction cascade. The classical studies of Terris and Steiner [3] first suggested that insulin degradation was itself a receptor-mediated process and it is now known that the insulin–receptor complex is rapidly internalized into the early endosome [4–7]. Maturation of the endosome leads to acidification, resulting in dissociation [8,9] of the insulin–receptor complex and allowing intra-endosomal insulin degradation with no transfer to the lysosome [10].

Earlier studies suggested that insulin-degrading enzyme (IDE; insulinase, EC 3.4.99.45) was the activity responsible for intracellular insulin degradation [11]. However, this hypothesis was based largely on evidence from experiments comparing IDE cleavage products with those from hepatocytes [5] and cell-free systems [12], although such products can be produced by a broad spectrum of metalloendoproteases [13]. Current evidence, such as the cytosolic [14] rather than endosomal location, wide substrate specificity [15] and sensitivity of the enzyme to both EDTA and *N*-ethylmaleimide (NEM) [16], suggests that IDE is not likely to be responsible for endosomal insulin processing. Alternative origins for endosomal insulin-degrading activity such as an insulin-specific endosomal protease [9], which is restricted to insulin-sensitive tissues, have also been suggested. However, the discovery that the amounts of different processing intermediates change with pH [17], implies that several enzymes with differing pH optima are active in insulin degradation. More recently, an acidic metalloendoprotease, differing from IDE by its lack of binding to both specific IDE antibodies and insulin, has been proffered as one of the degrading activities [18].

In the present study, insulin degradation within isolated rat liver endosomes was studied *in vitro* with the aid of three specifically labelled ^{125}I-insulin isomers (A14, B16 and B26). Chloroquine and 1,10-phenanthroline were used to minimize proteolysis during endosome preparation, and the manipulation of processing *in vitro* by Co^{2+} ions and 1,10-phenanthroline enabled the study of degradation intermediates and their time-dependent production. Structural and kinetic analyses of intermediates isolated from both intra- and extra-endosomal compartments has allowed the determination of major cleavage sites and the probable sequence of proteolytic events.

MATERIALS AND METHODS

Pig insulin suspension was purchased from Calbiochem and the zinc was removed as outlined by Christensen et al. [19]. Reverse-phase (RP) HPLC was performed on a Hypersil-BDS, 5 μm, C-18 column, 250 mm × 4.6 mm, fitted with an additional 10 mm guard cartridge of the same material and purchased from Shandon HPLC. The anti-insulin monoclonal antibodies 1E2 and 3B1 were produced in-house as described [20], and OXI005 was kindly provided by Novo Nordisk, Denmark. All other chemicals were purchased from Sigma Chemical Co. (Poole, Dorset, U.K.) and were of analytical grade.

Animals

Male Sprague–Dawley rats, 180–220 g body weight and fed *ad*

Abbreviations used: IDE, insulin-degrading enzyme; NEM, *N*-ethylmaleimide; RP HPLC, reverse-phase HPLC.

* To whom correspondence should be addressed.

libitum, were used throughout this study. All procedures involving animals were conducted in accordance with the British Home Office Animals Act, 1986.

Iodination

^{125}I-[A14]-insulin was prepared and purified as previously described [21]. Both ^{125}I-[B16]-insulin and ^{125}I-[B26]-insulin were prepared by a method based on [22]. Typically, 5 μl of 40 mM HCl containing 0.3 mg of pig insulin were mixed with 45 μl of 12 M urea. This mixture was reacted with 37 MBq of Na^{125}I (10 μl) in the presence of 2 μg of lactoperoxidase and 3.2 nmol of H_2O_2. The reaction was allowed to proceed at room temperature for 10 min before the addition of 40 μl of 0.4 M phosphate buffer, pH 7.2. Termination of the reaction after a total of 20 min was achieved by the addition of 20 μl of 0.24 % sodium metabisulphite. Finally the mixture was diluted with 100 μl of 5 % (w/v) BSA (Fraction V, RIA grade) in 0.4 M phosphate buffer, pH 7.2, to a volume of 250 μl, which was immediately separated by RP HPLC as described for the preparation of ^{125}I-[A14]-insulin [21].

Preparation of endosomes containing radiolabelled insulin

Approx. 10^6 Bq of specifically labelled ^{125}I-insulin in 0.5 ml of PBS was injected into anaesthetized rats via the hepatic portal vein over a 30 s period and the liver was removed after a further 2 min. After homogenization in 0.25 M sucrose/Hepes buffer (containing 10 mM Hepes buffer, pH 7.2, 1 mg/ml bacitracin and 2.5 mM NEM), an endosomal fraction was prepared by discontinuous sucrose gradient centrifugation [23]. This endosomal preparation contains 60 % of the recovered trichloroacetic acid-precipitable radiolabel, but less than 4 % of lysosomal enzymic activities [24]. The isolated endosomal population was subsequently washed free of cytosol by a 1:10 dilution in 10 mM Hepes buffer, pH 7.4, containing 0.1 M KCl and 2.5 mM NEM, and pelleted by centrifugation (100000 ***g*** at 4 °C for 30 min). In most experiments the homogenization and isolation buffers also contained 1 mM 1,10-phenanthroline to minimize uncontrolled endosomal degradation during vesicle preparation. In experiments where the kinetics of endosomal degradation were being investigated, endosomal degradation *in vivo* was controlled by administration of chloroquine to the rat. Rats were pretreated with chloroquine (20 mg/ml in PBS, pH 7.4) by intraperitoneal injection (at a dose of 5 mg/100 g body weight) 2 and 1 h before the start of the experiment along with the inclusion of chloroquine (1 mM) in all endosome isolation buffers. In a final step before the degradation *in vitro*, washed endosomes were resuspended in 50 mM ammonium acetate, pH 6.0, containing 1 mM 1,10-phenanthroline and dialysed for 30 min against the same buffer at 25 °C to remove any residual chloroquine.

Characterization of intra-endosomal degradation intermediates

Endosomes were prepared in the absence of 1,10-phenathroline and resuspended in 50 mM ammonium acetate, pH 6.0, before the endosomal degradation of internalized ^{125}I-insulin was initiated at 25 °C by the addition of 2.5 mM Co^{2+} ions and terminated at 0, 5, 15 or 30 min by the addition of 1,10-phenanthroline to a final concentration of 5 mM. A pH of 6.0 had been shown previously to be the optimum for endosomal degradation of internalized insulin [17]; this was confirmed in the present study (results not shown). Endosomes were separated from incubation medium by centrifugation (100000 ***g*** at 4 °C for 30 min) and the medium was retained for RP HPLC separation after freeze-drying. The entire endosomal contents were prepared for RP HPLC by endosomal lysis at pH 3.0 in the presence of 0.1 % Triton X-100 and 1 μM pig insulin as carrier, followed by separation from endosomal membranes by centrifugation (60000 ***g*** at 4 °C for 15 min). The degree of gross insulin degradation was determined by the proportion of trichloroacetic acid-soluble ^{125}I. Typically 100 μl of sample was combined with 50 μl of 5 % (w/v) BSA (Fraction V, RIA grade) and degradation was terminated by the immediate addition of 0.5 ml of 20 % (w/v) ice-cold trichloroacetic acid. After 15 min at 4 °C the samples were centrifuged (13000 ***g*** for 2 min) and the radioactivity in both the supernatants and pellets was determined in an LKB 1282 γ-counter.

Sulphitolysis

Isolated insulin degradation products were freeze-dried and derivatized by oxidative sulphitolysis [12]. Samples were rechromatographed under their original RP HPLC conditions and the elution profiles compared with the underivatized material. Oxidative sulphitolysis separates disulphide-bonded material by its conversion to the *S*-sulphonate derivative, thus identifying any intermediates containing both A- and B-chain elements.

Radiosequencing

Automated Edman degradation was performed with an Applied Biosystems (model 477) post-liquid sequencer. At the end of each cycle the anilinothiazolinone-derivatized amino acid was collected and any radioactivity released from the insulin degradation products was determined in an LKB 1282 γ-counter.

HPLC

RP HPLC separation of endosomal incubation medium and extracted endosomal contents was performed at a flow rate of 1 ml/min, in 0.1 M ammonium acetate buffer, pH 5.5, with an acetonitrile gradient. The precise changes in acetonitrile concentration (v/v) required to effect the separation of degradation intermediates were as follows: (1) 0–5 min at 0 %, (2) 5–20 min gradient rising to 8.45 %, (3) instantaneous rise to 28.5 %, (4) 20–40 min gradient rising to 32.5 %. These changes were followed by an increase in acetonitrile concentration to 50 % over 5 min, which was held for a further 5 min before returning to 0 % for a 20 min column re-equilibration.

The doublet (eluting at 26–27.5 min under these conditions) found in some samples of endosomes degrading ^{125}I-[B26]-insulin was resolved further by RP HPLC by column equilibration in buffer containing 10.4 % acetonitrile; separation was effected over 20 min with a linear gradient rising to 19.5 % acetonitrile.

Characterization of intra-endosomal processing intermediates by anti-insulin monoclonal antibodies

Initially, serial dilutions of the anti-insulin monoclonal antibodies 3B1, 1E2 and OXI005 were made to determine the concentration that would maximally bind approx. 350 Bq of either ^{125}I-[A14]-insulin or ^{125}I-[B16]-insulin. Degradation intermediates from the intra-endosomal degradation *in vitro* of these labelled insulins were separated by HPLC, collected and freeze-dried. Approx. 300 Bq of each intermediate was reconstituted in 50 mM sodium barbitone, pH 8.0, containing 0.5 % NaCl, 0.5 % BSA (Fraction V, RIA grade) and 0.01 % sodium azide before incubation in triplicate for 2 h at 25 °C with the appropriate concentration of anti-insulin antibody. Polyethylene glycol 8000 [15 % (w/v) in

PBS, pH 7.5, containing 0.25% γ-globulin and 0.05% (v/v) Tween-20 at 4 °C] was added and after 20 min was centrifuged (13000 ***g*** for 2 min at 4 °C) to effect the separation of bound and free labelled intermediates. The radioactivity in the pellets was determined in an LKB 1282 γ-counter and the amount of precipitable radioactivity expressed as a percentage of the total.

Compartmental analysis

The fluxes of ^{125}I-[A14]-insulin and its degradation intermediates from triplicate experiments were analysed in a compartmental model with the computer program SAAM II (RFKA, University of Washington, Seattle, WA, U.S.A.). After the separation of radioactive degradation intermediates from both endosomal contents and incubation medium (material escaping endosomes) by HPLC, the area under each radioactive peak was determined. The areas for all peaks of interest were summed and each peak representing a degradation intermediate was expressed as a percentage of this total. A matrix was constructed of the percentage in each peak with respect to time and the individual time courses for each peak were fitted simultaneously to each model under examination. Goodness of fit was estimated by comparison of the residual sums of squares.

RESULTS

Effect of Co^{2+} ions on endosomal insulin degradation inhibited by 1,10-phenanthroline

Previous studies [18] indicated that endosomal insulin-degrading activity is partly inhibited by the presence of 0.1 mM 1,10-phenanthroline and that the total activity returns in the presence of a 100-fold excess of Co^{2+} ions. In the present studies, preliminary experiments suggested that 1,10-phenanthroline in combination with Co^{2+} ions could be used to effect external control of endosomal insulin processing.

Endosomes containing internalized ^{125}I-[A14]-insulin were incubated at 25 °C for 35 min in either 50 mM ammonium acetate, pH 6.0, alone or in this buffer containing 1.0 mM 1,10-phenanthroline. Additions at 10 and 25 min of 2.5 mM Co^{2+} ions and/or 4 mM 1,10-phenanthroline respectively were made to endosomes incubated in the presence of 1 mM 1,10-phenanthroline. The disappearance of trichloroacetic acid-precipitable radiolabel was used as a marker for the intra-endosomal degradation of ^{125}I-[A14]-insulin.

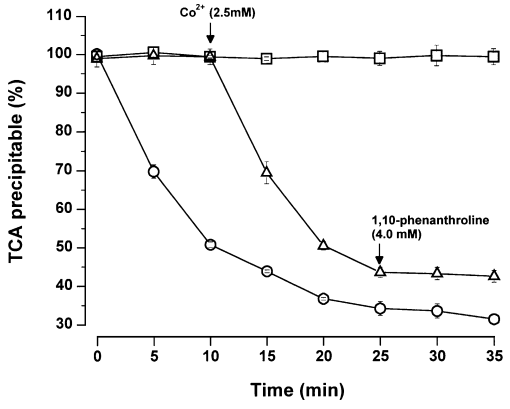

Figure 1 Effect of Co^{2+} and 1,10-phenanthroline on the endosomal degradation of ^{125}I-[A14]-insulin

Endosomes containing internalized ^{125}I-[A14]-insulin were incubated at 25 °C for 35 min in either 50 mM ammonium acetate buffer, pH 6.0, alone or in this buffer containing 1.0 mM 1,10-phenanthroline. The variation in trichloroacetic acid-precipitable radiolabel with time is shown. The points represent means ± S.D. ($n = 3$). Symbols: ○, degradation of internalized ^{125}I-[A14]-insulin at pH 6.0; □, degradation of internalized ^{125}I-[A14]-insulin at pH 6.0 in the presence of 1.0 mM 1,10-phenanthroline; △, degradation of internalized ^{125}I-[A14]-insulin in endosomes at pH 6.0, initially in the presence of 1.0 mM 1,10-phenanthroline with the addition of Co^{2+} (2.5 mM) at 10 min followed by the further addition of 1,10-phenanthroline (4.0 mM) at 25 min.

Figure 1 shows that 1 mM 1,10-phenanthroline completely inhibited endosomal insulin degradation. However, this inhibitory effect was not only reversed by a 1.5-fold excess of Co^{2+} ions but was re-established by a further 2-fold excess of chelating agent. Therefore alterations in the concentration of either 1,10-phenanthroline or cobalt can be used to control endosomal insulin degradation *in vitro*, permitting the analysis of processing intermediates produced within precise degradation time windows.

Isolation of processing intermediates from the endosomal incubation medium

Figure 2 shows the RP HPLC separation of radiolabelled products escaping into the incubation medium during the time-dependent degradation *in vitro* of internalized ^{125}I-insulin isomers. The intra-endosomal degradation of all three ^{125}I-insulin isomers (A14, B16 and B26) produced only one major product that exited from the endosome into the incubation medium. Further analysis, including comparison with internal calibration materials identified this product as ^{125}I-tyrosine. In both B16- and B26-labelled insulins, small amounts of both the intact insulin and other degradation intermediates also appeared in the incubation medium. However, the amounts of both insulin and these degradation intermediates remained constant, whereas ^{125}I-tyrosine production was time-dependent.

The possible presence of a specific carrier for ^{125}I-tyrosine within endosomes was examined by testing the ability of exogenous iodotyrosine to inhibit the efflux of the radiolabel. When endosomes containing internalized ^{125}I-[A14]-insulin were incubated in the presence of up to 100 mM unlabelled iodotyrosine, no difference in the rate of ^{125}I-tyrosine efflux was observed, indicating a diffusion-limited process rather than the presence of a specific carrier.

Isolation of degradation intermediates from endosomal contents

Figure 3 shows the RP HPLC separation of radiolabelled products found within the endosome after incubation for 5 min at 25 °C. The endosomes were prepared from livers of rats injected with each of the three labelled isomers. The intra-endosomal degradation of ^{125}I-[A14]-insulin (Figure 3A) showed the existence of five separate processing intermediates containing radiolabelled tyrosine. Separate control experiments in the absence of both 1,10-phenanthroline and Co^{2+} ions (results not shown) produced the same five intermediates, which indicates that these manipulations did not introduce any artifacts during endosomal insulin processing. The intermediates separated by RP HPLC included two (peaks 2 and 3) that are characteristic of ^{125}I-tyrosine and ^{125}I-[A14]-A-chain respectively, along with three other intermediates (peaks 1, 4 and 5) that did not co-elute with any calibration material.

The endosomal degradation of both ^{125}I-[B16]-insulin and ^{125}I-[B26]-insulin (Figures 3B and 3C respectively) showed the existence of three major processing intermediates that contained the radiolabel in addition to the starting material. In both cases a further intermediate, eluting after the intact insulin, was in too low an abundance to allow further analysis. However, the co-

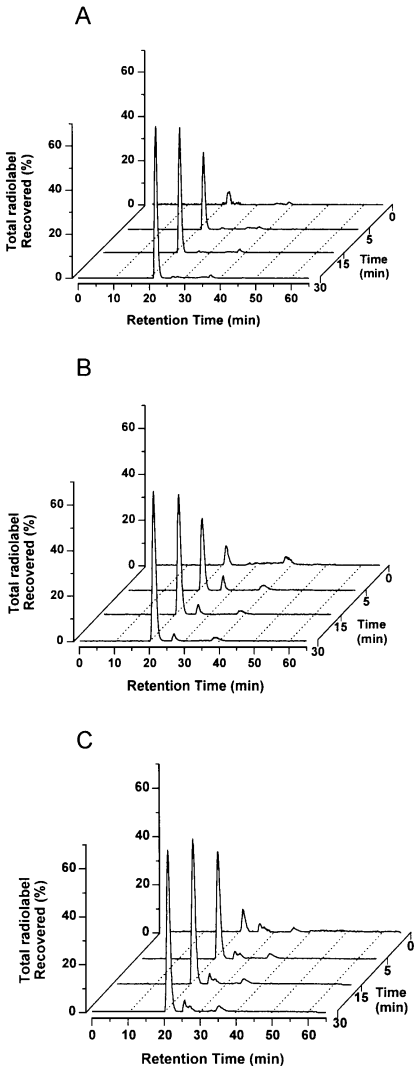

Figure 2 RP HPLC separation of radiolabelled insulin degradation products in endosomal incubation media

Radiolabelled degradation intermediates were isolated from incubation medium after the degradation of ^{125}I-insulin isomers *in vitro* (0, 5, 15 and 30 min incubations) ($n = 4$). In each panel the radioactivity for each intermediate is expressed as a percentage of total radiolabel for each time point and plotted against the HPLC retention time. (**A**) ^{125}I-[A14]-labelled insulin; (**B**) ^{125}I-[B16]-labelled insulin; (**C**) ^{125}I-[B26]-labelled insulin.

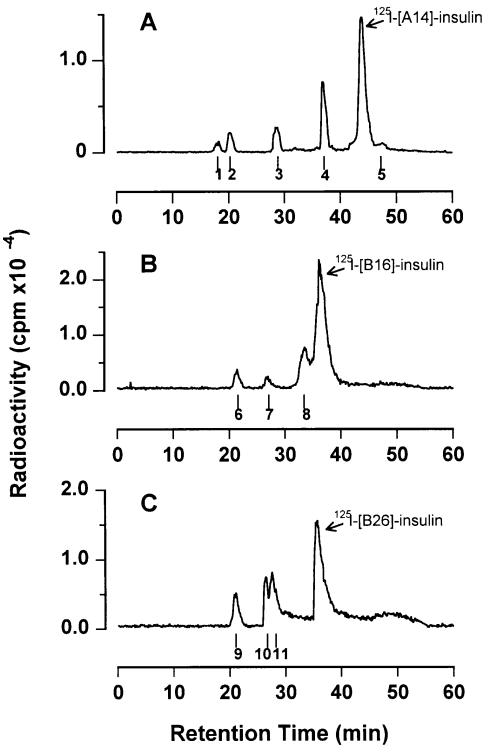

Figure 3 RP HPLC separation of radiolabelled insulin degradation intermediates found within endosomes after a 5 min incubation *in vitro*

Radiolabelled degradation intermediates were isolated from endosomes initially containing each ^{125}I-insulin isomer and were subsequently incubated *in vitro* for 5 min at 25 °C. Radioactivity is plotted against the RP HPLC retention time and is representative of four separate experiments. (**A**) ^{125}I-[A14]-labelled insulin; (**B**) ^{125}I-[B16]-labelled insulin; (**C**) ^{125}I-[B26]-labelled insulin. The reference numbers associated with each peak are used in the text for identification purposes in the subsequent characterization and kinetic studies.

elution of peaks 6 and 9 (Figures 3B and 3C respectively) with ^{125}I-tyrosine, identified ^{125}I-tyrosine as the final radiolabelled product of degradation from all three insulin isomers. The studies with both B16- and B26-labelled insulin revealed two further intermediates in each case. With ^{125}I-[B16]-insulin two peaks (peaks 7 and 8) eluting at 27 and 33 min respectively were found, whereas with ^{125}I-[B26]-insulin the intermediates (peaks 10 and 11) eluted as a doublet between 25 and 28 min. The constituents of this doublet were further resolved by RP HPLC after modification of the acetonitrile gradient as described in the Materials and methods section (results not shown).

Characterization of intra-endosomal processing intermediates

Individual peaks corresponding to the RP HPLC separation shown in Figure 3 were collected and subjected to further structural analysis by radiosequencing and oxidative sulphitolysis in conjunction with rechromatography (as described in the Materials and methods section). The results of this analysis together with the trichloroacetic acid solubility of the label in each peak are shown in Table 1.

In experiments where endosomes internalized ^{125}I-[A14]-insulin, intermediates 4 and 5 were found to be trichloroacetic acid-precipitable and to contain intact ^{125}I-[A14]-A-chain with associated B-chain elements. Although this was also true of intact insulin, the altered HPLC retention times for these intermediates were indicative of structural changes. In contrast, both intermediates 1 and 3 were soluble in trichloroacetic acid and contained no associated B-chain, whereas radiosequencing of these intermediates revealed the A14 label to be in the N-terminal position for intermediate 1 and at the 14th residue for intermediate 3. In addition, intermediate 3 co-eluted with intact ^{125}I-[A14]-A-chain under identical HPLC conditions.

With ^{125}I-[B16]-insulin as the starting material, intermediate 7, which was eluted earlier, was soluble in trichloroacetic acid, had no associated intact A-chain and contained the ^{125}I-tyrosine next to the N-terminus of the peptide. However, intermediate 8, the later-eluting intermediate, was not soluble in trichloroacetic acid, had associated A-chain elements and was not cleaved in the B-chain N-terminal to the ^{125}I-tyrosine.

With ^{125}I-[B26]-insulin, in addition to the starting material and ^{125}I-tyrosine, the end product of degradation, two peptides were

Table 1 Characteristics of intra-endosomal insulin degradation intermediates

Retention times from both before and after oxidative sulphitolysis (Ox. sulph.) after RP HPLC of intermediates, are shown, as well as results from direct radiosequencing analysis and assessment of trichloroacetic acid (TCA) solubility of the radiolabel. Symbols: + and − denote (> 75%) either TCA-soluble or -insoluble respectively.

	Intermediate no.	Identity	Label position from N-terminus	HPLC retention time (min)		TCA soluble
				Native	Ox. sulph.	
A14	1		1	19.5	19.5	+
	2	^{125}I-Tyr	1	21.5	21.5	+
	3		14	28.5	28.5	−
	4		14	35.0	28.5	−
		^{125}I-[A14]-insulin	14	38.5	28.5	−
	5		14	42.5	28.5	−
B16	6	^{125}I-Tyr	1	21.5	21.5	+
	7		2	27.0	27.0	+
	8		16	33.0	45.0	−
		^{125}I-[B-16]-insulin	16	35.0	45.0	−
B26	9	^{125}I-Tyr	1	21.5	21.5	+
	10		1	26.0	*	+
	11		2	27.5	*	+
		^{125}I-[B-26]-insulin	26	35.5	43.0	−

* No data owing to insufficient material.

resolved by RP HPLC that eluted as a doublet (peaks 10 and 11). After further resolution of these peaks under altered gradient conditions, both intermediates were found to be soluble in trichloroacetic acid; the labelled tyrosine was either at the N-terminus or next to the N-terminus.

Characterization of intra-endosomal processing intermediates by anti-insulin monoclonal antibodies

Intra-endosomal degradation products produced from both A14- and B16-labelled insulin isomers were further characterized by immunoprecipitation (as described in the Materials and methods section) with a panel of three anti-insulin monoclonal antibodies of known epitope specificity [20]. All antibodies recognized epitopes within the insulin B-chain: 3B1 and 1E2 recognized residues B9–20 and B1–15 respectively, whereas OXI005 recognized the C–terminal tail (B27–30). The abilities of the various antibodies to precipitate the radiolabelled intermediates are shown in Table 2.

In addition to iodotyrosine, neither intermediates 1 or 3 were precipitated by any of the antibodies used, confirming the absence of B-chain. Conversely, intermediate 5 was precipitated by all the antibodies in the panel and was therefore indistinguishable from intact iodoinsulin. Intermediates 4 and 8 were precipitated by antibodies 3B1 and 1E2 but not by OX1005, indicating the presence of a B-chain fragment from B1 to between B20 and B26. The lack of precipitation of intermediate 7 by OXI005 indicates that at least the last four residues of the B-chain were missing, whereas precipitation by 3B1 suggests the presence of some of the central B-chain region B7–20. The structural data suggesting that B15 is the N-terminal residue in this peptide are supported by its partial precipitation (50%) by 1E2.

The kinetics of intra-endosomal degradation intermediate production

Figure 4 shows the HPLC traces indicating the time courses for appearance and disappearance of the various intermediates found within endosomes after incubation for up to 30 min. One of the main features for each isomer is that even at the start of the incubation there were significant amounts of trichloroacetic acid-precipitable degradation. This is presumably the result of endosomal processing occurring *in vivo* between the administration of the radiolabelled insulin and homogenization of the liver. With ^{125}I-[A14]-insulin (Figure 4A), appreciable amounts (15–20% of the total radioactivity) of intermediates 4 and 5 could be seen at zero time, but none of intermediates 1, 2 or 3. Therefore intermediates 4 and 5 must have been generated first in the proteolytic sequence. Similarly, with the ^{125}I-[B16]-insulin, intermediate 8 was present at zero time and therefore must have been produced first. With ^{125}I-[B26]-insulin, intermediate 11 was present in large amounts at zero time and decreased with time, whereas peak 10 seemed to be in steady state.

Table 2 Determination of insulin epitopes within degradation intermediates

Results of immunoprecipitation of insulin degradation intermediates by a panel of anti-insulin monoclonal antibodies. Symbols: + and − denote either successful (> 70%) or unsuccessful (< 10%) immunoprecipitation respectively. The epitope recognized by the antibody is indicated in parentheses.

			Antibody ...	Immunoprecipitation		
^{125}I-insulin	no.	Identity		3B1 (B9–20)	1E2 (B1–15)	OXI005 (B27–30)
A14	1			−	−	−
	2	^{125}I-Tyr		−	−	−
	3	^{125}I-[A14]-A chain		−	−	−
	4			+	+	−
		^{125}I-[A14]-insulin		+	+	+
	5			+	+	+
B16	6	^{125}I-Tyr		−	−	−
	7			+	±	−
	8			+	+	−
		^{125}I-[B16]-insulin		+	+	+

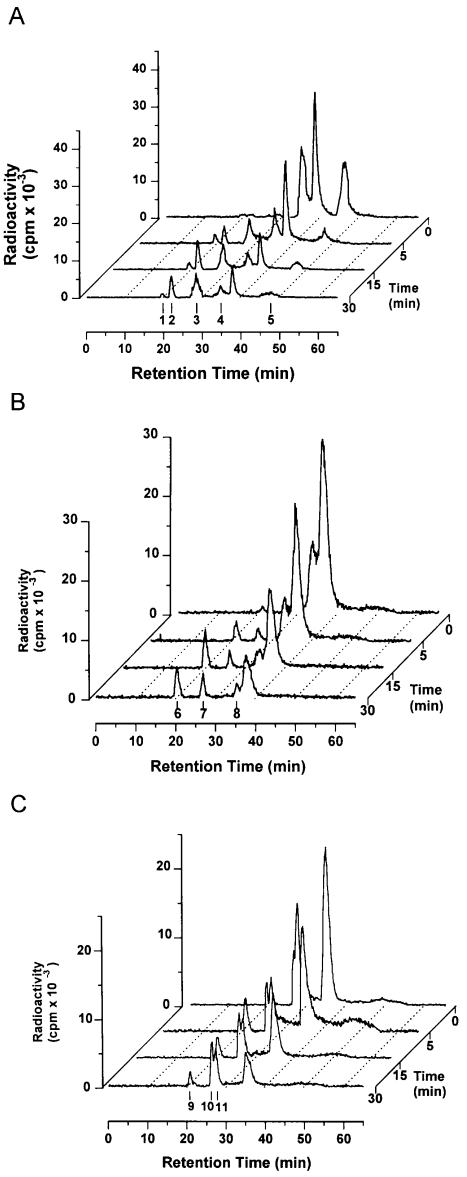

Figure 4 RP HPLC separation of radiolabelled insulin degradation intermediates found within endosomes

Radiolabelled degradation intermediates were isolated from endosomal contents after the degradation of ^{125}I-insulin isomers *in vitro* (0, 5, 15 and 30 min incubations). Radioactivity is plotted against the HPLC retention time and is representative of four separate experiments. (**A**) ^{125}I-[A14]-labelled insulin; (**B**) ^{125}I-[B16]-labelled insulin; (**C**) ^{125}I-[B26]-labelled insulin.

To simplify the kinetic analysis, endosomes containing internalized ^{125}I-[A14]-insulin were isolated from rats after pretreatment with chloroquine as described in the Materials and methods section to minimize insulin degradation during the isolation of endosomes [10,23]. Degradation of the internalized insulin was then allowed to proceed under the control of the reversible inhibitor 1,10-phenanthroline. Aliquots were removed at timed intervals up to 30 min during degradation, and intermediates were isolated by RP HPLC from both the incubation medium and endosomal contents. The variation with time of the percentage of total radioactivity found in each peak is shown in Table 3.

The results show that the presence of both chloroquine and 1,10-phenanthroline *in vivo* during endosomal isolation did not inhibit insulin degradation to the point where the radiolabel was associated only with intact ^{125}I-[A14]-insulin. Indeed, the zero time point of degradation *in vitro* shows that approx. 11 % of the radiolabelled material was associated with intermediate 4. On the initiation of degradation the amount of intact insulin showed a rapid decline, whereas the appearance of iodotyrosine (peak 2), although rapid, was not equivalent to insulin's disappearance. Intermediate 4 was the only intermediate present at time zero, indicating that it was the first product of ^{125}I-[A14]-insulin cleavage. This intermediate rose to a plateau between 2 and 5 min before decreasing rapidly to 3 % of the radioactivity after 30 min of degradation. Intermediate 5, although never present in large amounts, reached a maximum at 2 min before dropping to zero after 15 min, suggesting its production early in the degradation sequence. Therefore if the intra-endosomal degradation of insulin were to follow a linear sequence, intermediate 4 would be the precursor for intermediate 5. The two remaining intermediates, 1 and 3, both rose slowly to a relatively low level with a maximum at 15 min and then decreased gradually. However, intermediate 3 did initially rise faster than intermediate 1, suggesting an earlier formation. The amount of iodotyrosine shown in Table 3 is the sum of that in the incubation medium and that found within the endosome. However, the amount of ^{125}I-tyrosine in the incubation medium rose as degradation proceeded, whereas the ^{125}I-tyrosine concentration within the endosome reached a maximum after 5 min and thereafter remained constant (results not shown). Thus the kinetics suggests that for a linear pathway of degradation of ^{125}I-[A14]-insulin to occur it must follow the route: intact insulin → intermediate 4 → intermediate 5 → intermediate 3 → intermediate 1 → iodotyrosine. However, the structural evidence shown in Tables 1 and 2 indicates that intermediate 5 was produced directly from intact insulin and might be the precursor for intermediate 4 rather than its cleavage product. This contradiction suggests that the degradation pathway might not be linear but more complex.

To examine further the possible sequence of proteolytic events, the kinetic data were subjected to compartmental modelling and analysis. Initially, the data relating to intact insulin, ^{125}I-tyrosine and the four other intermediates of ^{125}I-[A14]-insulin degradation were assembled into various linear sequences of proteolysis. Compartmental analysis was used to identify the sequence of intermediates that would produce optimal agreement between the experimental and modelled data. The sequence (Scheme 1A) had the smallest residual sums of squares (211) for all the linear sequences studied. However, Figure 5A shows the existence of a systematic deviation between the fitted lines and the experimental data, which is largest for both the disappearance of ^{125}I-[A14]-insulin and the appearance of ^{125}I-tyrosine. The structural information about the degradation intermediates was then used to suggest other suitable degradation sequences including more complex parallel pathways. The sequence of proteolytic events depicted in Scheme 1B gave the best fit of all the combinations tested and the residual sums of squares was significantly reduced, to 23 ($P < 0.001$), from the higher value seen with the linear sequence. Figure 5B shows the improved agreement between the experimental data sets and the fitted lines for the more complex dual-pathway model.

Table 4 shows the rate constants for the dual-pathway model of ^{125}I-[A14]-insulin degradation. These rate constants fall into two categories, with those for the pathway via intermediate 5 to ^{125}I-tyrosine greater than those for the other sequential route via intermediates 4, 3 and 1 to ^{125}I-tyrosine. The fastest step in the degradation of ^{125}I-[A14]-insulin is the conversion of intermediate 5 to iodotyrosine, whereas the slowest and therefore rate-limiting process is the production of intermediate 3 from intermediate 4.

Table 3 The fluxes of ^{125}I-insulin and radiolabelled proteolytic intermediates during endosomal degradation *in vitro*

Proportions of total radioactive counts from various radiolabelled degradation intermediates isolated from the intra-endosomal degradation of ^{125}I-[A14]-insulin. The relative amounts of each intermediate were determined from the peak areas of RP HPLC elution profiles; these are expressed as a percentage of the total radioactivity ($n = 4$) and shown as means ± S.D.

		Proportion of total radioactive counts (%)					
Time (min)	Peak ... Identity ...	1	2 (I-Tyr)	3 (A-chain)	4 (deshexapeptide insulin)	– ^{125}I-[A14]-insulin	5
0		0.0 ± 0.0	0.0 ± 0.0	0.0 ± 0.0	11.5 ± 0.5	88.5 ± 0.5	0.0 ± 0.0
2		0.5 ± 0.5	11.0 ± 0.0	3.0 ± 0.0	17.5 ± 0.5	62.0 ± 1.0	6.0 ± 1.0
5		2.5 ± 0.5	25.0 ± 3.0	7.0 ± 1.0	18.0 ± 0.0	44.5 ± 2.5	3.0 ± 1.0
15		6.5 ± 1.5	42.5 ± 2.5	8.0 ± 0.0	8.0 ± 1.0	36.5 ± 1.5	0.0 ± 0.0
30		4.5 ± 1.5	55.0 ± 1.0	3.5 ± 0.5	3.0 ± 2.0	33.5 ± 2.5	0.0 ± 0.0

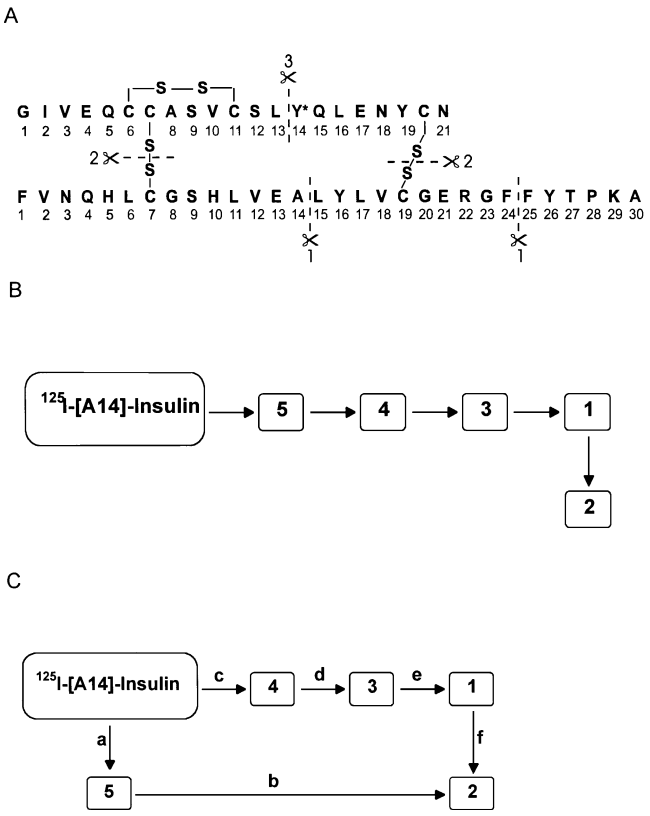

Scheme 1 Diagram of the primary structure of insulin together with representations of the compartmental models

(**A**) Primary structure of insulin with the suggested cleavage points indicated by broken lines together with their order of occurrence indicated numerically. (**B**) Compartmental diagram for a linear sequence of proteolytic cleavages; (**C**) dual pathway of degradation. The numbers on compartmental models in (**B**) and (**C**) refer to the intermediates as identified in Figure 3. The letters in (**C**) refer to rate constants determined in the compartmental analysis and presented in Table 4.

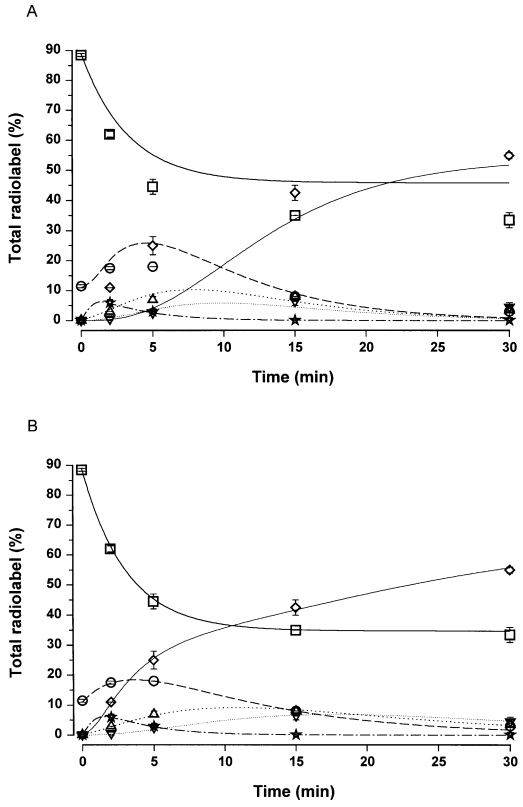

Figure 5 Kinetics of intermediate production during ^{125}I-[A-14]-insulin degradation

The relative amounts of each radiolabelled intermediate, determined as the percentage of total radioactivity for each time point and plotted against time. The points represent the means ± S.E.M. of four experiments in each case. The following lines correspond to the computer-generated fit, and the symbols represent the corresponding experimental results: close dots, ▽, intermediate 1; solid line, ◇, intermediate 2; spaced dots, △, intermediate 3; broken line, ○, intermediate 4; solid line, □, ^{125}I-[A14]-insulin; dot-dashed line, ☆, intermediate 5. (**A**) Data with fitted lines representing a linear sequence of proteolysis (Scheme 1B); (**B**) the same data fitted to a more complex dual pathway of degradation (Scheme 1C).

DISCUSSION

Intra-endosomal insulin degradation is completely inhibited by the chelating agent 1,10-phenanthroline (1.0 mM) but this inhibition can be completely reversed by an excess of Co^{2+} ions. Use of this inhibitor in the isolation of endosomes from chloroquine-pretreated rats results in minimal proteolysis of the internalized insulin. Degradation of internalized insulin within these endosomes can be initiated *in vitro* by the addition of excess Co^{2+} ions and halted after a defined period by the re-establishment

Table 4 Rate constants for the proteolytic cleavages generating radiolabelled degradation intermediates

Rate constants are shown for the proteolytic cleavages described in the dual-pathway model that are responsible for generating the radiolabelled degradation intermediates. The letters refer to the rate constants as identified in Scheme 1B.

Rate constant	Intermediate generated	Value (%/s)
a	5	0.207 ± 0.009
b	2	1.114 ± 0.080
c	4	0.118 ± 0.008
d	3	0.106 ± 0.004
e	1	0.137 ± 0.009
f	2	0.149 ± 0.015

of an excess of 1,10-phenanthroline. This technique has enabled an examination of the kinetics of insulin degradation intermediates produced by the action of proteases contained within the endosome and has two advantages over the methodologies used in previous studies. First, it allows the detection of transient intermediates that might be missed if appearing early in the degradation sequence. Secondly, it allows a study of the kinetics of peak appearance and disappearance from which additional evidence can be obtained about the sequence of proteolytic events. When compared with HPLC analysis of radiolabelled endosomal contents in the absence of either 1,10-phenanthroline or Co^{2+} ions, we found no evidence that these agents caused an alteration of the degradation pathway.When monitoring degradation by following the behaviour of the ^{125}I label, intra-endosomal degradation of all three labelled insulin isomers proceeds by first generating trichloroacetic acid-precipitable intermediates and then trichloroacetic acid-soluble peptides, which are rapidly processed through to monoiodotyrosine. This is in contrast with some previous studies [12,25], which have suggested that peptide intermediates from ^{125}I-[B26]-insulin degradation are able to cross the endosomal membrane. It is probable that larger peptides can escape only if the endosomes are damaged during isolation. We have previously shown by using Ag^{2+} ions [10] that the endosomes prepared by the method of [23] are largely intact. Our experiments show that iodotyrosine is the ultimate radiolabelled product of endosomal insulin degradation and is the only radiolabelled degradation product able to escape the endosome. This implies that insulin is degraded to its constituent amino acids within the endosome. The intra-endosomal concentration of ^{125}I-tyrosine reaches a maximum after 5 min of degradation and then reaches a plateau. This suggests that the passage of ^{125}I-tyrosine across the endosomal membrane is not rate-limiting. In addition, the inability of exogenous mono-iodotyrosine to inhibit the efflux of ^{125}I-tyrosine indicates that efflux is diffusion-limited rather than dependent on a specific carrier [26]. Examination of the data in Table 1 shows that some insulin degradation products are in fact trichloroacetic acid-precipitable. Thus a measurement of the disappearance of precipitability by trichloroacetic acid is only an indicator of gross proteolytic cleavage. However, the values obtained for the individual rate constants (Table 4) indicate that the appearance of trichloroacetic acid-soluble products represents the slowest step in the overall degradation process. Thus the kinetics of the appearance of trichloroacetic acid-soluble radioactivity will indicate the value of the rate-limiting step for insulin degradation.

In common with previous studies [12,17,25] we have shown that endosomal insulin degradation begins with proteolytic cleavages within the B-chain before the A-chain is attacked. HPLC analysis of endosomal contents after endocytosis of insulin labelled at A14 or B16 revealed three intermediates containing intact A-chain. One of these intermediates was identified as A-chain itself. The other two intermediates contained A-chain with fragments of B-chain attached by the disulphide bridges. All three specifically labelled isomers produced an intermediate that was more hydrophobic than the intact native isomer. In the B-16 and B-26 isomers the yield of this intermediate was too low to permit further characterization. However, the corresponding intermediate isolated from ^{125}I-[A14]-insulin degradation (peak 5) was indistinguishable from intact insulin by all the analytical techniques used except for its characteristically longer retention time. An indication as to the possible identity of this species comes from the use of the B16 isomer, which produces an intermediate (peak 7) that loses radiolabel after two cycles of radiosequencing, indicating a cleavage between B-chain residues 14 and 15. Cleavage of native insulin at this point would produce an intermediate with very similar characteristics to native insulin because the molecule would be held together by the interchain disulphide bonds. Cleavage of the disulphide bond would then produce intermediate 7.

Only two peptide intermediates, 10 and 11, were isolated from the degradation of ^{125}I-[B26]-insulin in sufficient quantities for further analysis. Radiosequencing analysis has for the first time confirmed the identities of these previously isolated [12,25] intermediates as the B-chain C-terminal pentapeptide (B26–30) and hexapeptide (B25–30) respectively. Use of specific antibodies suggests that intermediates 4 and 8 lack at least the last four C-terminal amino acids from the B-chain. Thus identification of the hexapeptide (B25–30) as an insulin degradation intermediate suggests that the identity of both intermediates 4 and 8 is radiolabelled deshexapeptide insulin produced by a cleavage at B24-25. In addition, intermediate 7 shows no reaction with antibody X1005, indicating the absence of the last four C-terminal amino acids. However, it also shows only partial precipitation with antibody 1E2 (recognizing B1–15), indicating that rather more of the C-terminus might be absent. Thus this intermediate may be derived, after disulphide reduction, from degradation routes initiated by cleavage at either B14-15 or B24-25.

The earliest study to isolate the B-chain C-terminal hexapeptide (B25–30) and pentapeptide (B26–30) from the degradation of ^{125}I-[B26]-insulin [12] suggested the parallel production of the peptides. However, the kinetic fluxes of these two intermediates show a fall in the amounts of hexapeptide and a corresponding rise in the levels of the pentapeptide, suggesting a sequential cleavage process. Because monoiodotyrosine is the only other radiolabelled product isolated from ^{125}I-[B26]-insulin degradation, a sequential cleavage of the hexapeptide to produce first the pentapeptide (B26–30) and then liberate tyrosine by an aminopeptidase-like activity is suggested.

Previous studies investigating the endosomal degradation of ^{125}I-[B26]-insulin *in vivo* [12] and *in vitro* [17,25] have suggested a cleavage at B16-17. However, two of these studies [12,25] did not identify intermediates directly but inferred this conclusion by comparison with intermediates generated by IDE degradation. Because IDE is almost certainly not involved in physiologically relevant insulin degradation, this inference is suspect. Although the other study did suggest a B16-17 cleavage as a result of intermediate radiosequencing, the authors expressed doubts over the purity of their B-26-labelled insulin. It is possible that a B16-17 cleavage would result in a product not resolvable from intact ^{125}I-[B16]-insulin under our HPLC conditions. This might then be subject to the combined action of the activity giving rise

to the cleavage at B14-15 and the amino peptidase activity, thus producing iodotyrosine. However, we can find no evidence of a B16-17 cleavage with any of our radiolabelled insulins and suggest from the results obtained with ^{125}I-[B16]-insulin that B14-15 is the initial proteolytic site in this region (B7–19) of the insulin molecule.

Examination of the proteolytic process with respect to the A-chain has been possible with the study of ^{125}I-[A14]-insulin degradation. Apart from ^{125}I-tyrosine and the B-chain-containing intermediates the study of this isomer's degradation reveals two further intermediates, 1 and 3, that contain no associated B-chain. Further analysis of intermediate 3, including its co-elution with ^{125}I-[A14]-A-chain, suggests its identity as intact A-chain, therefore implying the presence of an intra-endosomal disulphide-reducing activity. We have only partly identified the other A-chain peptide, intermediate 1, but have established that the peptide comprises fewer than eight residues with the A14 tyrosine at the N-terminal position. Intermediate 1 is not the A-chain octapeptide (A14–21) because the specifically iodinated A14 isomer of this peptide does not co-elute with intermediate 1 under identical HPLC conditions (results not shown). Both the structural and kinetic analyses suggest that after disulphide reduction the intact A-chain is cleaved in two places, one of which is A13-14, to release intermediate 1. Further processing of intermediate 1 by an aminopeptidase-like activity results in ^{125}I-tyrosine production.

Insulin degradation is not only initiated by an endoprotease cleaving the B-chain at B14-15 and B24-25; the subsequent degradation of intact A-chain (at A13-14) is also the result of such an activity. The requirement for either a large aliphatic residue (Leu at B15) or a non-polar aromatic amino acid residue (Phe at B25) is characteristic of the action of a neutral or alkaline metalloendoprotease [13]. Such activities were first described for bacterial enzymes [27], which tend to utilize zinc in a stabilizing role [28], but the catalytic activity of the alkaline enzyme in particular is increased by the replacement of Zn^{2+} by Co^{2+} ions [28]. The B24-25 cleavage generates hexapeptide, which is the precursor for pentapeptide and subsequently the production of ^{125}I-tyrosine, whereas the A13-14 cleavage produces a peptide whose degradation again liberates ^{125}I-tyrosine. In both cases there is a sequential loss of N-terminal amino acids, which is indicative of an aminopeptidase activity. The degradation of ^{125}I-[B26]-insulin reveals a relative increase in amounts of both pentapeptide and hexapeptide, suggesting a slower rate of cleavage by the aminopeptidase than the metalloendoprotease. It has not yet been possible to identify unequivocally any of the enzymic activities involved in the endosomal degradation of insulin. Several laboratories have isolated an aminopeptidase activity (gp160) from the GLUT-4-containing vesicles of insulin-responsive tissues [29,30]. However, liver contains the GLUT-2 glucose transporter, which is not translocated in response to stimulation by insulin.

A compartmental analysis of the kinetics of appearance and disappearance of the radiolabelled intermediates allowed us to discriminate between various alternative pathways for the sequence of degradation. A completely ordered sequential pathway and a random non-ordered pathway could be eliminated immediately on the basis of an extremely poor fit of the data to either of these models. After examination of a number combinations it was found that the most probable sequence of events involved a dual pathway as illustrated in Scheme 1C. Most of the intermediates observed were derived from a basically ordered sequence, involving an initial cleavage in the B-chain at 24-25 followed by disulphide reduction, then A-chain cleavage at 13-14, and finally aminopeptidase activity to produce iodotyrosine. The alternative arm of the pathway generates intermediate 5 via cleavage at B14-15 and then leads straight to iodotyrosine production. Although other intermediates must be present in this pathway, their steady-state concentration is too low for them to be detected.

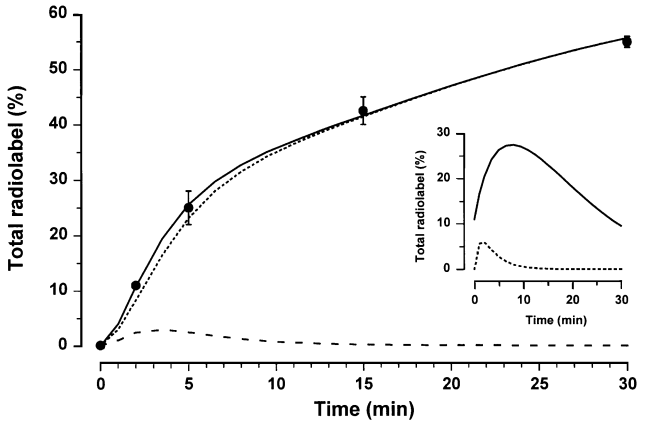

Figure 6 The contribution of each arm of the dual pathway to the overall degradation of insulin

Result of a computer simulation of the contribution to total production of ^{125}I-tyrosine (●, solid line) from the upper (dotted line) and lower (broken line) pathways of Scheme 1C. The rate constants used were those obtained at best fit and shown in Table 4. Inset: flux through each of the two pathways, represented as the percentage of the total radiolabel present in each pathway at the indicated time.

The rate constants obtained for the dual pathway model suggest that the rate-limiting step in the production of [^{125}I]iodotyrosine is the production of A-chain from the des-hexapeptide intermediate. This might be by reduction of the disulphide bonds themselves, which is also likely to result from enzymic activity, although such activities have not yet been identified in hepatic endosomal vesicles. However, endosomal reduction of interchain disulphide bonds has been described for the entry and activation of diphtheria toxin in Vero cells [31]. If the dual-pathway model suggested by the kinetics is an accurate reflection of the true events in endosomal insulin degradation, then it is likely that a particular pathway is blocked or favoured as a result of conformational changes bought about by the initial cleavage point.

The compartmental model also allows a visualization of the amounts of insulin being degraded by each pathway, as shown in Figure 6. Apart from very early time points, almost all the iodotyrosine is obtained through the top pathway in Scheme 1C, i.e. via the B24-25 cleavage. Thus in practice most of the degradation seems to proceed via an ordered sequential pathway. Consequently this implies that inhibition of the B24-25 cleavage might effectively block endosomal degradation. Some initial studies have been conducted with an insulin analogue substituted with His for Phe at the B25 position [32]. Endosomal degradation of this analogue is significantly slower than that of native insulin, and the analogue also has an extended duration of action with respect to insulin-stimulated glucose uptake in 3T3-L1 adipocytes.

Summary of the sequence of intra-endosomal insulin proteolysis

Our data suggest that endosomal processing of insulin is initially achieved by a metalloendoprotease that cleaves the molecule in the B-chain towards the C-terminus at B24-25 and/or in the

centre region at B14-15. Cleavage at B24-25 might preclude subsequent cleavage at B14-15. The B24-25 cleavage produces a hexapeptide, which is sequentially proteolysed by an aminopeptidase. The major part of the hormone, deshexapeptide insulin, has its interchain disulphide bonds reduced, thus liberating A-chain. The A-chain is subsequently cleaved at A13-14 by a carboxypeptidase, and somewhere C-terminal of A15 to create a peptide fragment from which tyrosine is liberated.

We thank Dr N. J. Crowther for his considerable help in performing the immunoprecipitation assays, and Novo Nordisk for the anti-insulin monoclonal antibody OX1005. We thank the Medical Research Council for funding this research.

REFERENCES

1 Ballotti, R., Kowalski, A., White, M. F., LaMarchand-Brustel, Y. and Van Obberghen, E. (1987) Biochem. J. **241**, 99–104
2 Khan, M. N., Baquiran, G., Brule, C., Burgess, J., Foster, B., Bergeron, J. J. M. and Posner, B. I. (1989) J. Biol. Chem. **264**, 12931—12940
3 Terris, S. and Steiner, D. F. (1975) J. Biol. Chem. **250**, 8389–8398
4 Carpentier, J. L., Fehlmann, M., Van Obberghen, E., Gorden, P. and Orci, L. (1985) Diabetes **34**, 1002–1007
5 Duckworth, W. C., Hamel, F. G., Peavy, D. E., Liepnieks, J. J., Ryan, M. P., Hermodson, M. A. and Frank, B. H. (1988) J. Biol. Chem. **263**, 1826–1833
6 Sonne, O. (1988) Physiol. Rev. **68**, 1129–1196
7 Levy, J. R. and Olefsky, J. M. (1987) Endocrinology (Baltimore) **121**, 2075–2086
8 Doherty, J., Kay, D., Lai, W., Posner, B. and Bergeron, J. (1990) J. Cell Biol. **110**, 35–42
9 Backer, J., Kahn, C. and White, M. (1990) J. Biol. Chem. **265**, 14828–14835
10 Pease, R. J., Smith, G. D. and Peters, T. J. (1987) Eur. J. Biochem. **164**, 251–257
11 Duckworth, W. (1988) Endocrin. Rev. **9**, 319–345
12 Hamel, F. G., Posner, B. I., Bergeron, J. J., Frank, B. H. and Duckworth, W. C. (1988) J. Biol. Chem. **263**, 6703–6708
13 Jochen, A. and Berhanu, P. (1987) Biochem. Biophys. Res. Commun. **142**, 205–212
14 Hari, J., Shii, K. and Roth, R. A. (1987) Endocrinology (Baltimore) **120**, 829–831
15 Muller, D., Baumeister, H., Buck, F. and Richter, D. (1991) Eur. J. Biochem. **202**, 285–292
16 Ding, L., Becker, A. B., Suzuki, A. and Roth, R. A. (1992) J. Biol. Chem. **267**, 2414–2420
17 Clot, J. P., Janicot, M., Fouque, F., Desbuquois, B., Haumont, P. Y. and Lederer, F. (1990) Mol. Cell. Endocrinol. **72**, 175–178
18 Authier, F., Rachubinski, R. A., Posner, B. I. and Bergeron, J. J. (1994) J. Biol. Chem. **269**, 3010–3016
19 Christensen, J. R., Smith, G. D. and Peters, T. J. (1985) Cell Biochem. Funct. **3**, 13–19
20 Crowther, N. J., Xiao, B., Jorgensen, P. N., Dodson, G. G. and Hales, C. N. (1994) Prot. Engng. **7**, 137–144
21 Rideout, J. M., Smith, G. D., Lim, C. K. and Peters, T. J. (1985) Biochem. Soc. Trans. **13**, 1225–1226
22 Frank, B. H., Peavy, D. E., Hooker, C. S. and Duckworth, W. C. (1983) Diabetes **32**, 705–711
23 Pease, R. J., Smith, G. D. and Peters, T. J. (1985) Biochem. J. **228**, 137–146
24 Pease, R. J., Sharp, G., Smith, G. D. and Peters, T. J. (1984) Biochim. Biophys. Acta **774**, 56–66
25 Hamel, F. G., Mahoney, M. J. and Duckworth, W. C. (1991) Diabetes **40**, 436–443
26 Andersson, H. C., Kohn, L. D., Bernardini, I., Blom, H. J., Tietze, F. and Gahl, W. A. (1990) J. Biol. Chem. **265**, 10950–10954
27 Feder, J. (1967) Biochemistry **6**, 2088–2093
28 Morihara, K. (1974) Adv. Enzymol. Relat. Areas. Mol. Biol. **41**, 179–243
29 Kandror, K. V., Yu, L. and Pilch, P. F. (1994) J. Biol. Chem. **269**, 30777–30780
30 Mastick, C. C., Aebersold, R. and Lienhard, G. E. (1994) J. Biol. Chem. **269**, 6089–6092
31 Rolband, G. C., Williams, J. F., Webster, N. J. G., Hsu, D. and Olefsky, J. M. (1993) Biochemistry **32**, 13545–13550
32 Seabright, P. J., Tikerpae, J. and Smith, G. D. (1996) Diabetic Med. **13** (4), S18-S19 (abstract)

Received 5 July 1996/23 August 1996; accepted 6 September 1996